

Quantum frequency down-conversion of bright amplitude-squeezed states

Dehuan Kong, Zongyang Li, Shaofeng Wang, Xuyang Wang, and Yongmin Li*

State Key Laboratory of Quantum Optics and Quantum Optics Devices, Institute of Opto-Electronics, Shanxi University, Taiyuan 030006, China

*yongmin@sxu.edu.cn

Abstract: We demonstrate experimentally the quantum frequency down-conversion of a bright amplitude-squeezed optical field via a high efficiency difference frequency generation process. 532 nm amplitude-squeezed light with squeezing of 1.0 dB is successfully translated to 810 nm amplitude-squeezed light with squeezing of 0.8 dB. The effects of amplitude and phase fluctuations of the pump field on the frequency conversion are investigated both theoretically and experimentally. It is shown that the quantum frequency down-conversion is insensitive to small amplitude fluctuations of the pump field at the optimal conversion point. However, the phase fluctuations of the pump field can lead to increase of noise in the phase quadrature of the down-converted field. To eliminate the additive phase noise, a dual frequency down-converter which utilizing common pump field is proposed and demonstrated.

©2014 Optical Society of America

OCIS codes: (270.5585) Quantum information and processing; (190.4410) Nonlinear optics, parametric processes; (130.7405) Wavelength conversion devices.

References and links

1. S. Tanzilli, W. Tittel, M. Halder, O. Alibart, P. Baldi, N. Gisin, and H. Zbinden, "A photonic quantum information interface," *Nature* **437**(7055), 116–120 (2005).
2. A. P. VanDevender and P. G. Kwiat, "Quantum transduction via frequency upconversion," *J. Opt. Soc. Am. B* **24**(2), 295–299 (2007).
3. H. J. Kimble, "The quantum internet," *Nature* **453**(7198), 1023–1030 (2008).
4. L. J. Ma, O. Slattery, and X. Tang, "Single photon frequency up-conversion and its applications," *Phys. Rep.* **521**(2), 69–94 (2012).
5. G. Giorgi, P. Mataloni, and F. De Martini, "Frequency Hopping in Quantum Interferometry: Efficient Up-Down Conversion for Qubits and Ebits," *Phys. Rev. Lett.* **90**(2), 027902 (2003).
6. M. A. Albota, F. N. C. Wong, and J. H. Shapiro, "Polarization-independent frequency conversion for quantum optical communication," *J. Opt. Soc. Am. B* **23**(5), 918–924 (2006).
7. H. Takesue, "Erasing Distinguishability Using Quantum Frequency Up-Conversion," *Phys. Rev. Lett.* **101**(17), 173901 (2008).
8. M. T. Rakher, L. J. Ma, O. Slattery, X. Tang, and K. Srinivasan, "Quantum transduction of telecommunications-band single photons from a quantum dot by frequency upconversion," *Nat. Photonics* **4**(11), 786–791 (2010).
9. H. Takesue, "Single-photon frequency down-conversion experiment," *Phys. Rev. A* **82**(1), 013833 (2010).
10. N. Curtz, R. Thew, C. Simon, N. Gisin, and H. Zbinden, "Coherent frequency-down-conversion interface for quantum repeaters," *Opt. Express* **18**(21), 22099–22104 (2010).
11. Y. Ding and Z. Y. Ou, "Frequency downconversion for a quantum network," *Opt. Lett.* **35**(15), 2591–2593 (2010).
12. M. T. Rakher, L. J. Ma, M. Davanço, O. Slattery, X. Tang, and K. Srinivasan, "Simultaneous Wavelength Translation and Amplitude Modulation of Single Photons from a Quantum Dot," *Phys. Rev. Lett.* **107**(8), 083602 (2011).
13. S. Zaske, A. Lenhard, and C. Becher, "Efficient frequency downconversion at the single photon level from the red spectral range to the telecommunications C-band," *Opt. Express* **19**(13), 12825–12836 (2011).
14. K. De Greve, L. Yu, P. L. McMahon, J. S. Pelc, C. M. Natarajan, N. Y. Kim, E. Abe, S. Maier, C. Schneider, M. Kamp, S. Höfling, R. H. Hadfield, A. Forchel, M. M. Fejer, and Y. Yamamoto, "Quantum-dot spin-photon entanglement via frequency downconversion to telecom wavelength," *Nature* **491**(7424), 421–425 (2012).
15. S. Ramelow, A. Fedrizzi, A. Poppe, N. K. Langford, and A. Zeilinger, "Polarization-entanglement-conserving frequency conversion of photons," *Phys. Rev. A* **85**(1), 013845 (2012).
16. C. J. McKinstrie, L. Mejling, M. G. Raymer, and K. Rottwitz, "Quantum-state-preserving optical frequency conversion and pulse reshaping by four-wave mixing," *Phys. Rev. A* **85**(5), 053829 (2012).

17. H. J. McGuinness, M. G. Raymer, C. J. McKinstrie, and S. Radic, "Quantum Frequency Translation of Single-Photon States in a Photonic Crystal Fiber," *Phys. Rev. Lett.* **105**(9), 093604 (2010).
18. Y. O. Dudin, A. G. Radnaev, R. Zhao, J. Z. Blumoff, T. A. B. Kennedy, and A. Kuzmich, "Entanglement of Light-Shift Compensated Atomic Spin Waves with Telecom Light," *Phys. Rev. Lett.* **105**(26), 260502 (2010).
19. S. L. Braunstein and P. V. Loock, "Quantum information with continuous variables," *Rev. Mod. Phys.* **77**(2), 513–577 (2005).
20. A. Furusawa and N. Takei, "Quantum teleportation for continuous variables and related quantum information processing," *Phys. Rep.* **443**(3), 97–119 (2007).
21. X. B. Wang, T. Hiroshima, A. Tomita, and M. Hayashi, "Quantum information with Gaussian states," *Phys. Rep.* **448**(1-4), 1–111 (2007).
22. T. C. Ralph and P. K. Lam, "A bright future for quantum communications," *Nat. Photonics* **3**(12), 671–673 (2009).
23. M. D. Reid, P. D. Drummond, W. P. Bowen, E. G. Cavalcanti, P. K. Lam, H. A. Bachor, U. L. Andersen, and G. Leuchs, "The Einstein-Podolsky-Rosen paradox: From concepts to applications," *Rev. Mod. Phys.* **81**(4), 1727–1751 (2009).
24. C. Weedbrook, S. Pirandola, R. García-Patrón, N. J. Cerf, T. C. Ralph, J. H. Shapiro, and S. Lloyd, "Gaussian quantum information," *Rev. Mod. Phys.* **84**(2), 621–669 (2012).
25. J. M. Huang and P. Kumar, "Observation of quantum frequency conversion," *Phys. Rev. Lett.* **68**(14), 2153–2156 (1992).
26. C. E. Vollmer, C. Baune, A. Sambrowski, T. Eberle, V. Händchen, J. Fiurášek, and R. Schnabel, "Quantum up-conversion of squeezed vacuum states from 1550 to 532 nm," *Phys. Rev. Lett.* **112**(7), 073602 (2014).
27. M. D. Levenson, R. M. Shelby, A. Aspect, M. Reid, and D. F. Walls, "Generation and detection of squeezed states of light by nondegenerate four-wave mixing in an optical fiber," *Phys. Rev. A* **32**(3), 1550–1562 (1985).
28. R. M. Shelby, M. D. Levenson, S. H. Perlmutter, R. G. DeVoe, and D. F. Walls, "Broad-band parametric deamplification of quantum noise in an optical fiber," *Phys. Rev. Lett.* **57**(6), 691–694 (1986).
29. P. Galatola, L. A. Lugiato, M. G. Porreca, P. Tombesi, and G. Leuchs, "System control by variation of the squeezing phase," *Opt. Commun.* **85**(1), 95–103 (1991).
30. Z. Y. Ou, "Efficient conversion between photons and between photon and atom by stimulated emission," *Phys. Rev. A* **78**(2), 023819 (2008).

1. Introduction

Quantum interface capable of transferring quantum states between different central frequencies is a necessary component for quantum information processing [1,2]. Such quantum-state-preserving frequency conversion (QFC) enables seamless connection of quantum devices that operate at different optical frequencies [3]. For instance, in a quantum communication network, efficient mapping between quantum light fields at wavelengths $\sim 0.8 \mu\text{m}$ and $\sim 1.5 \mu\text{m}$ is essential for the connection of a quantum memory device consists of alkaline atoms and a quantum communication device where a low-loss telecom fiber is employed as the quantum channel. QFC also allows for optimal single photon detection by converting near infrared photons to visible or near visible range photons where high efficiency and low noise silicon single photon detectors are commercially available. Such single photon frequency up-conversion detector has found key applications in the implementation of quantum key distribution systems and characterization of single photon and entangled photon sources [4].

Nonlinear optical parametric process is one of the most efficient mechanisms for the implementation of QFC. Single photon and entangled photon QFC have been achieved using three-wave mixing in a nonlinear optical crystal [5–16], four-wave mixing in a photonic crystal fiber [17], and in a cold Rb vapor [18]. Stimulated by the high efficiency in preparing and manipulating the quantum states as well as the unconditionalness, continuous variables (CV) regime utilizing continuous quadrature amplitudes of the quantized electromagnetic field has emerged as an alternative way for developing novel quantum information processing protocols [19–24]. Using sum-frequency process, the up-conversions of nonclassical intensity correlations [25] and squeezed vacuum state [26] have been observed. However, the complementary process, frequency down-conversion of nonclassical CV quantum states which is essential in quantum information processing hasn't been achieved so far.

For QFC based on three-wave mixing, strong pump field is a prerequisite to ensure a high fidelity QFC. In reality, the pump laser always suffers from amplitude and phase fluctuations far above the quantum noise limit (QNL), especially at the low-frequency range. For

instance, semiconductor lasers and fiber lasers are currently convenient approaches to provide high power coherent emission for their compact size and versatility, but both suffer from large excess noises. In CV regime, two approaches are currently utilized to measure the quadratures of optical fields: balanced homodyne detection (BHD) and self-homodyne measurements by a frequency-dependent reflection of the optical field [27–29]. Both methods required that the signal field has a bright carrier. For the BHD, the bright carrier is used to calibrate the relative phase between the signal field and the local oscillator (LO) by two-beam interference. For the latter one, the bright carrier component plays the role of LO. In both cases, the noisy pump field can modulate the signal field and transfer a portion of signal carrier to the signal sideband modes on which CV quantum states are situated. This process deteriorates the fidelity of CV QFC.

In this paper, we investigate the effects of excess pump noises on CV QFC of bright quantum states, and experimentally demonstrate the first quantum frequency down-conversion of a bright amplitude-squeezed state from 532 nm to 810 nm. The presented QFC utilizes pump-enhanced difference frequency generation (DFG) process and features high photon conversion efficiency (85%), low conversion noises, and wideband conversion characteristics. The demonstrated scheme provides an effective way for faithful frequency conversion of bright CV quantum states with noisy pump field. The ability of down-conversion of CV quantum states demonstrated in our work combined with that of up-conversion of CV quantum states demonstrated in previous works make a two-way CV QFC possible which are critical in quantum communication. Our work also verifies that DFG can transfer faithfully more complex quantum states between different frequencies besides single photon state.

2. Influence of amplitude and phase fluctuations of the pump field on QFC

The Hamiltonian of the DFG process in the interaction picture is described by $\hat{H} = i\hbar k A_p^* \hat{a}_i \hat{a}_c^\dagger - i\hbar k^* A_p \hat{a}_i^\dagger \hat{a}_c$, here k is the nonlinear coupling constant, A_p is the strong pump field and described by a c number, \hat{a}_i and \hat{a}_c stand for the input and down-converted light fields, the angular frequencies of the pump, input, and down-converted fields satisfy the energy conservation relationship: $\omega_i = \omega_p + \omega_c$. Under the undepleted pump approximation the evolution of the system gives [30]

$$\hat{a}_{c,out} = \hat{a}_{c,in} \cos(|kA_p|\tau) + e^{-i\phi} \hat{a}_{i,in} \sin(|kA_p|\tau), \quad (1)$$

$$\hat{a}_{i,out} = \hat{a}_{i,in} \cos(|kA_p|\tau) - e^{i\phi} \hat{a}_{c,in} \sin(|kA_p|\tau), \quad (2)$$

where $e^{i\phi} = k^* A_p / |kA_p|$ and τ is the interaction time. When the pump field is treated as a perfectly coherent monochromatic field with a stabilized amplitude and phase, one can obtain a complete quantum state frequency conversion at $|kA_p|\tau = \pi/2$ and $\phi = 0$, because $\hat{a}_{c,out} = \hat{a}_{i,in}$, $\hat{a}_{i,out} = -\hat{a}_{c,in}$.

In the following we reconsider the QFC where a noisy pump laser is employed. The pump offset is defined as $\Delta = |kA_p|\tau - \pi/2$, substitute $\pi/2 + \Delta$ for $|kA_p|\tau$, Eqs. (1) and (2) can be rewritten as

$$\hat{a}_{c,out} = -\hat{a}_{c,in} \sin \Delta + e^{-i\phi} \hat{a}_{i,in} \cos \Delta, \quad (3)$$

$$\hat{a}_{i,out} = -\hat{a}_{i,in} \sin \Delta - e^{i\phi} \hat{a}_{c,in} \cos \Delta. \quad (4)$$

To analyze the fluctuation of $\hat{a}_{c,out}$, the amplitudes of optical fields are expanded in terms of mean fields and small fluctuations. Consider the special case of $\Delta \ll \pi/2$ and keep only the first-order terms, the fluctuation of $\hat{a}_{c,out}$ can be obtained from Eq. (3)

$$\begin{aligned} \delta\hat{a}_{c,out} = & -\delta\hat{a}_{c,in} \sin \Delta - \delta\Delta \cdot \hat{a}_{c,in} \cos \Delta \\ & + e^{-i(\phi)} \left[\delta\hat{a}_{i,in} \cdot \cos \Delta - i\delta\phi \cdot \hat{a}_{i,in} \cos \Delta - \delta\Delta \cdot \hat{a}_{i,in} \sin \Delta \right]. \end{aligned} \quad (5)$$

To assure the same quadrature is being compared in all input and output fields, the quadratures are defined as

$$\begin{aligned} \hat{X}_c = \frac{1}{2}(\hat{a}_c e^{i(\phi)} + \hat{a}_c^\dagger e^{-i(\phi)}) \quad \hat{X}_i = \frac{1}{2}(\hat{a}_i + \hat{a}_i^\dagger) \quad X_p = \frac{1}{2}(A_p e^{-i(\phi_p)} + A_p^* e^{i(\phi_p)}) \\ \hat{Y}_c = \frac{1}{2i}(\hat{a}_c e^{i(\phi)} - \hat{a}_c^\dagger e^{-i(\phi)}) \quad \hat{Y}_i = \frac{1}{2i}(\hat{a}_i - \hat{a}_i^\dagger) \quad Y_p = \frac{1}{2i}(A_p e^{-i(\phi_p)} - A_p^* e^{i(\phi_p)}) \end{aligned} \quad (6)$$

where $e^{i\phi_p} = A_p/|A_p|$ is the phase of the pump field, $\hat{X}(X)$ and $\hat{Y}(Y)$ are the amplitude and phase quadratures of the optical fields, respectively.

By using the definitions of ϕ , ϕ_p , Δ , X_p , and Y_p , one can obtain

$$\delta\Delta \approx \frac{\pi}{2} \frac{\delta X_p}{|A_p^0|}, \quad \delta\phi = \delta\phi_p \approx \delta Y_p / |A_p|, \quad (7)$$

where A_p^0 satisfies $|kA_p^0| \tau - \pi/2 = 0$. It follows from Eqs. (5) and (6), the quadrature fluctuations of the down-converted field can be given by

$$\begin{aligned} \delta\hat{X}_{c,out} = \frac{1}{2} \left[\delta\hat{a}_{c,out} e^{i(\phi)} + \delta\hat{a}_{c,out}^\dagger e^{-i(\phi)} \right] \\ = -\sin \Delta \cdot \delta\hat{X}_{c,in} - \delta\Delta \cdot \cos \Delta \cdot \hat{X}_{c,in} + \cos \Delta \cdot \delta\hat{X}_{i,in} - \delta\Delta \cdot \sin \Delta \cdot \hat{X}_{i,in} + \delta\phi_p \cdot \cos \Delta \cdot \hat{Y}_{i,in}, \end{aligned} \quad (8)$$

$$\begin{aligned} \delta\hat{Y}_{c,out} = \frac{1}{2i} \left[\delta\hat{a}_{c,out} e^{i(\phi)} - \delta\hat{a}_{c,out}^\dagger e^{-i(\phi)} \right] \\ = -\sin \Delta \cdot \delta\hat{Y}_{c,in} - \delta\Delta \cdot \cos \Delta \cdot \hat{Y}_{c,in} + \cos \Delta \cdot \delta\hat{Y}_{i,in} - \delta\Delta \cdot \sin \Delta \cdot \hat{Y}_{i,in} - \delta\phi_p \cdot \cos \Delta \cdot \hat{X}_{i,in}. \end{aligned} \quad (9)$$

From Eqs. (8) and (9), the quadrature variance can be determined as

$$\begin{aligned} N_{\hat{X}_{c,out}} = & \left\langle \left(\delta\hat{X}_{c,out} \right)^2 \right\rangle \\ = & \left\langle \left(\delta\hat{X}_{c,in} \right)^2 \right\rangle \sin^2 \langle \Delta \rangle + \left\langle \left(\delta\hat{X}_{i,in} \right)^2 \right\rangle \cos^2 \langle \Delta \rangle + \cos^2 \langle \Delta \rangle \cdot \left\langle (\delta\Delta)^2 \right\rangle \cdot \left\langle \left(\hat{X}_{c,in} \right)^2 \right\rangle \\ & + \left\langle (\delta\phi_p)^2 \right\rangle \cdot \cos^2 \langle \Delta \rangle \cdot \left\langle \left(\hat{Y}_{i,in} \right)^2 \right\rangle + \sin^2 \langle \Delta \rangle \cdot \left\langle (\delta\Delta)^2 \right\rangle \cdot \left\langle \left(\hat{X}_{i,in} \right)^2 \right\rangle, \end{aligned} \quad (10)$$

$$\begin{aligned} N_{\hat{Y}_{c,out}} = & \left\langle \left(\delta\hat{Y}_{c,out} \right)^2 \right\rangle \\ = & \left\langle \left(\delta\hat{Y}_{c,in} \right)^2 \right\rangle \sin^2 \langle \Delta \rangle + \left\langle \left(\delta\hat{Y}_{i,in} \right)^2 \right\rangle \cos^2 \langle \Delta \rangle + \cos^2 \langle \Delta \rangle \cdot \left\langle (\delta\Delta)^2 \right\rangle \cdot \left\langle \left(\hat{Y}_{c,in} \right)^2 \right\rangle \\ & + \sin^2 \langle \Delta \rangle \cdot \left\langle (\delta\Delta)^2 \right\rangle \cdot \left\langle \left(\hat{Y}_{i,in} \right)^2 \right\rangle + \left\langle (\delta\phi_p)^2 \right\rangle \cdot \cos^2 \langle \Delta \rangle \cdot \left\langle \left(\hat{X}_{i,in} \right)^2 \right\rangle. \end{aligned} \quad (11)$$

We assume the initial down-converted field $\hat{a}_{c,in}$ is in a vacuum state, the input signal field $\hat{a}_{i,in}$ is relatively intense ($\sqrt{\langle(\delta\hat{X}_{i,in})^2\rangle}, \sqrt{\langle(\delta\hat{Y}_{i,in})^2\rangle} \ll \langle\hat{X}_{i,in}\rangle$), and the strong pump field satisfies $\sqrt{\langle(\delta\phi_p)^2\rangle}, \sqrt{\langle(\delta A_p)^2\rangle} \ll \langle A_p\rangle$. By using these assumptions, the third and fourth terms of Eqs. (10) and (11) are much smaller than other terms and can be disregarded. Inserting Eq. (7) into Eqs. (10) and (11), we have

$$N_{\hat{X}_{c,out}} = \langle(\delta\hat{X}_{c,in})^2\rangle \sin^2 \langle\Delta\rangle + \langle(\delta\hat{X}_{i,in})^2\rangle \cos^2 \langle\Delta\rangle + \sin^2 \langle\Delta\rangle \frac{\pi^2 P_{i,in} \omega_p}{4 P_p^0 \omega_s} \langle(\delta X_p)^2\rangle, \quad (12)$$

$$N_{\hat{Y}_{c,out}} = \langle(\delta\hat{Y}_{c,in})^2\rangle \sin^2 \langle\Delta\rangle + \langle(\delta\hat{Y}_{i,in})^2\rangle \cos^2 \langle\Delta\rangle + \cos^2 \langle\Delta\rangle \frac{P_{i,in} \omega_p}{P_p \omega_s} \langle(\delta Y_p)^2\rangle, \quad (13)$$

where $P_{i,in}$ and P_p are input signal and pump power, P_p^0 is the pump power at the point of complete conversion, ω_s and ω_p are angular frequencies of the signal and pump fields. It is convenient to express the parameters Δ in terms of the ones that are accessible experimentally $\Delta = (\pi/2)(|A_p|/|A_p^0| - 1) = (\pi/2)(\sqrt{P_p/P_p^0} - 1)$.

The added amplitude quadrature and phase quadrature noise variances of the down-converted field can be given by

$$\begin{aligned} N'_{\hat{X}_{c,out}} &= N_{\hat{X}_{c,out}} - \langle(\delta\hat{X}_{i,in})^2\rangle \\ &= \sin^2 \langle\Delta\rangle \left(\langle(\delta\hat{X}_{c,in})^2\rangle - \langle(\delta\hat{X}_{i,in})^2\rangle \right) + \sin^2 \langle\Delta\rangle \frac{\pi^2 P_{i,in} \lambda_s}{4 P_p^0 \lambda_p} \langle(\delta X_p)^2\rangle, \end{aligned} \quad (14)$$

$$\begin{aligned} N'_{\hat{Y}_{c,out}} &= N_{\hat{Y}_{c,out}} - \langle(\delta\hat{Y}_{i,in})^2\rangle \\ &= \sin^2 \langle\Delta\rangle \left(\langle(\delta\hat{Y}_{c,in})^2\rangle - \langle(\delta\hat{Y}_{i,in})^2\rangle \right) + \cos^2 \langle\Delta\rangle \frac{P_{i,in} \lambda_s}{P_p \lambda_p} \langle(\delta Y_p)^2\rangle. \end{aligned} \quad (15)$$

From Eqs. (14) and (15), it is evident that excess amplitude and phase noises can be added to the down-converted quantum state, and the induced excess noises depend on the experimental parameters Δ , $P_{i,in}/P_p^0$, $\langle(\delta X_p)^2\rangle$, and $\langle(\delta Y_p)^2\rangle$. However, when the pump field intensity is adjusted at the point of complete conversion ($\Delta = 0$), the QFC is insensitive to the small amplitude noises of the pump field, while it is not the case for the phase noises. The QFC is more sensitive to phase fluctuations than to amplitude fluctuations of the pump field in the region of $\Delta \ll \pi/2$. The carrier power of the signal field also affects the excess noises in the down-converted field where lower signal carrier power leads to less excess noises.

3. QFC of 532 nm bright amplitude-squeezed state and its dependence on the pump power

The schematic diagram of the experimental setup is shown in Fig. 1. The quantum states (squeezing state and coherent state) are prepared via the second harmonic generation process driven with a single-frequency continuous wave Nd:YVO4/KTP laser. Bright amplitude squeezed green light at 532 nm was generated by an external cavity-enhanced singly resonant frequency doubler where a 10-mm MgO doped periodically poled lithium niobate

(MgOPPLN) was utilized, and 1.0 dB of amplitude squeezing was observed at a broadband sideband frequency. The coherent state is prepared by strong attenuation of the generated green light.

The quantum state frequency down-conversion system consists of two identical pump-enhanced DFG devices in which a 1550 nm single frequency fiber laser is used as the pump source. Each DFG device consists of two concave mirrors with 30 mm radii of curvature and a 30-mm-long MgOPPLN nonlinear medium. The input coupler was coated for high transmission at 532 and 810 nm and partial transmission ($\sim 4\%$) at 1550 nm. The output coupler was coated for high reflectivity at 1550 nm and high transmission at 532 and 810 nm. Such cavity designs ensure broadband quantum frequency conversion as well as high circulating intracavity pump power, which is crucial for the transfer of wide-band input quantum states. The bandwidth of the QFC is determined in principle by the phase-matching bandwidth of the nonlinear crystal which is on the order of 1 nm. After the frequency down-conversion, the generated 810 nm fields are separated from the residual 532 nm and 1550 nm light fields by a series of optical filters.

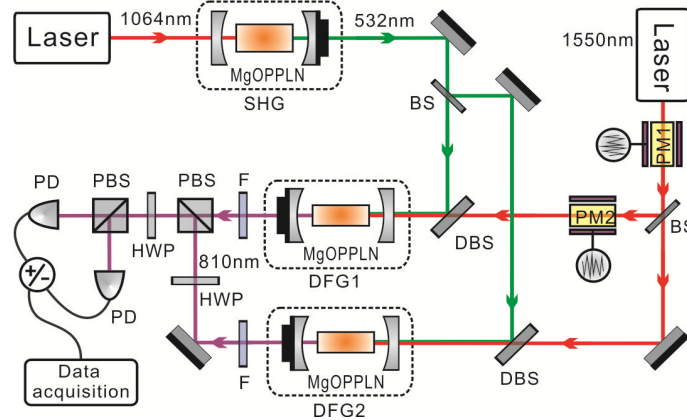


Fig. 1. Schematic of the experimental setup. SHG, second harmonic generation; BS, beamsplitter; DBS, dichroic beamsplitter; DFG1, DFG2, difference frequency generation device; HWP, half waveplate; PBS, polarizing beamsplitter; F, filters; PD, photodiode, PM1, PM2, phase modulators.

Figure 2(a) shows the classical DFG efficiency of a weak 532 nm input field (0.8 mW) versus the pump power at 1550 nm. A maximum photon-number conversion efficiency of $85 \pm 0.2\%$ was achieved at a pump power of 348 mW and further increase of the pump intensity results a strong back conversion from the generated 810 nm light to the original 532 nm light. The high efficiency here is critical to a high fidelity QFC, because any imperfect conversion will lead to the addition of vacuum noise and contaminate the down-converted quantum state. The nonideal conversion efficiency comes from the losses of the cavity mirrors and nonlinear crystal, also the finite beam size of the pump comparing with that of the signal. Figure 2(b) shows the output power of the down-converted 810 nm light at different 532 nm powers from 15 to 1000 μW . The results verified that the DFG is linear versus the input power in a range of 2 orders of magnitude.

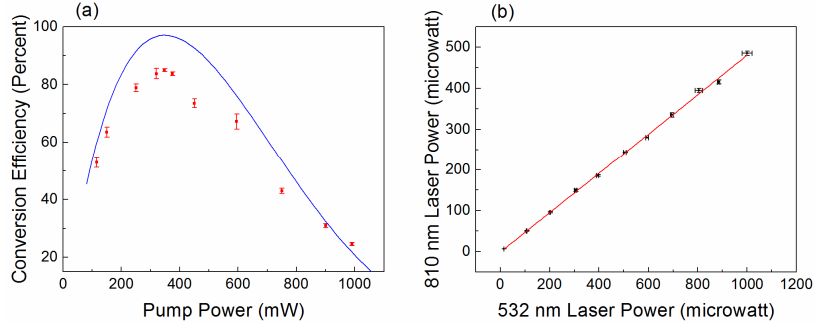


Fig. 2. (a) Frequency down-conversion efficiency of a weak 532 nm input field versus the 1550 nm pump power. The solid square is the experimental values and the solid line is the theoretical fitting. (b) Output power of 810 nm light as a function of input 532 nm power. The solid square is the experimental data and the solid line is a linear fit to the data.

To achieve the frequency down-conversion of 532 nm amplitude-squeezed state, only DFG1 was participated (the pump field intensity is set at the maximum parametric conversion efficiency point) where bright squeezed state with mean power of 14 mW is injected. A self-homodyne detection was used to measure the amplitude noise spectrum of the input and output quantum states. As shown in Figs. 3(a) and 3(b), the input 532 nm light with ~ 1 dB squeezing is transferred to an 810 nm light with ~ 0.8 dB of squeezing. This means that the DFG here unconditionally transfers the sub-Poissonian photon statistics of the 532 nm squeezed state to that of the 810 nm squeezed state. The frequency conversion of the squeezed state can be modeled with a linearized Gaussian channel such that $\hat{X}_{810} = \sqrt{\eta} \hat{X}_{532} + \sqrt{1-\eta} \hat{X}_{vac} + D$. Here D is independent noise on the channel with variance V_{add} , η is the transmissivity with $\eta = \eta_t \eta_{fc} \eta_d$, where $\eta_t = 0.89$ is the optical propagation transmission, $\eta_{fc} = 0.85$ is the frequency-conversion efficiency, and $\eta_d = 0.84$ is the detection efficiency for the 810 nm optical field. Using the experimental values of Fig. 3(a) and set $V_{add} = 0$, we obtain the theoretical squeezing spectrum at 810 nm (the solid line of Fig. 3(b)) which is in good agreement with the observed value. This means that the degradation of the squeezing is mainly due to the linear loss coming from the optical propagation transmission and imperfect frequency-conversion efficiency. Negligible amount of excess noise was introduced during the QFC process.

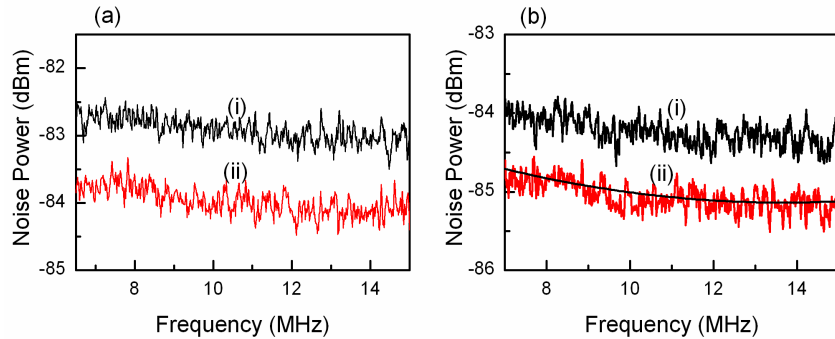


Fig. 3. Amplitude quadrature noise spectrum for the input squeezed state at 532 nm (a) and for the frequency down-converted quantum state at 810 nm (b), the solid line is the theoretical fitting. (i) Quantum noise limit; (ii) Amplitude quadrature noise. The resolution and video bandwidths of the spectrum analyzer are 120 kHz and 30 Hz, respectively.

When the pump field intensity is detuned away from the maximum conversion efficiency point, the excess amplitude noises of the pump will transfer to the down-converted field and

contaminates the QFC process as we have shown theoretically in Section II. Figure 4 shows the added amplitude noise to the 810 nm field as a function of the pump offset Δ at the analysis frequency of 8 MHz. The solid square denotes the experimental data and the solid line is the theoretical simulations by using Eq. (14) and the experimental parameters (the amplitude noise of the 1550 nm pump field was measured to be 29.3 QNL units at 8 MHz for detected power of 6 mW). From Fig. 4, when the pump offset Δ increases from 0 to 0.1, excess amplitude noise of the 810 nm field appears and increases accordingly. For $|\Delta| = 0.1$, excess noise of around 0.8 QNL unit was added. The experimental values are in reasonable agreement with the theoretical predictions.

4. Phase noise cancellation

In Section II it is proven that the phase fluctuations of the pump field can induce the unwanted phase noise in the down-converted field. To verify this, two DFG devices are employed to translate the signal field and the LO respectively. A 532 nm vacuum state which lies in 8 MHz sideband around the carrier (the mean power of the carrier is 140 μ W) was used as the input quantum state. The output quantum state at 810 nm was detected by a BHD. The generated photocurrents were subtracted, preamplified, and further mixed with a sinusoidal reference of 8 MHz, followed by a low pass filter with a bandwidth of 200 kHz. The filtered signals which are proportional to the field quadrature values of the sideband modes were sampled at different LO phases from 0 to 2π which are determined from the interference fringe between the LO and the bright signal field.

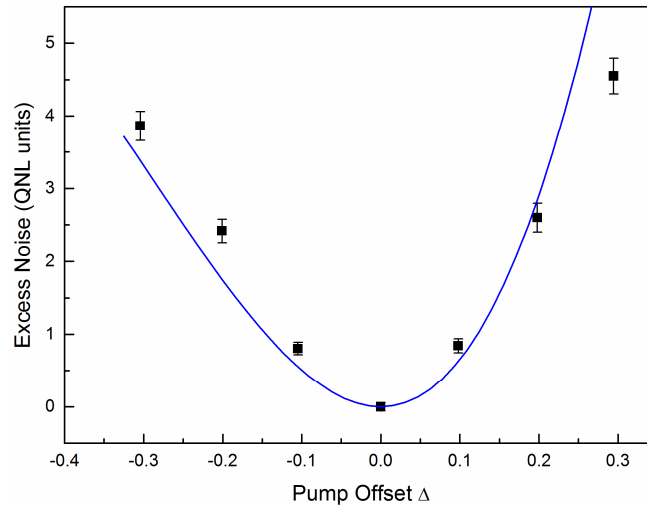


Fig. 4. The added amplitude noise to the 810 nm light field versus the pump offset Δ . The solid square is the experimental data and the solid line is the theoretical simulations.

As before, the pump power of both DFGs is adjusted precisely to the point of the maximum conversion efficiency, whereas the pump field of DFG1 was phase modulated by white noises (PM2) with a bandwidth of 100 MHz and modulation depth of 45 mrad. This simulates the situation that only the signal field is down-converted with a noisy pump, and the non-modulated down-converted LO here is only for characterization of the quadratures of the signal field. Figure 5(a) shows the Wigner functions of the down-converted 810 nm quantum state reconstructed from a sample of 1000000 quadrature-phase pairs. The amplitude quadrature variance of the 810 nm state is at the vacuum state level, while the phase quadrature is enlarged significantly from the vacuum state with a normalized variance of 13.6 dB (22.9 QNL on a linear scale) due to the phase noise of the pump beam (Fig. 5(c)).

If we utilize a dual DFG and translate the LO at the same time using the same noisy pump field as that used for the QFC of input quantum state, in the new phase reference of the

down-converted LO, the classical phase noise of the field $\hat{a}_{c,out}$ coming from the pump field can be cancelled completely in principle. Such cancellation is valid over the whole frequency range including very low frequency down to DC. As shown in Fig. 5(b), when the pump fields of the two DFGs were phase modulated simultaneously by white noises using PM1 (the white noises here has the same parameters as that used for PM2 before), the added phase noises from the pump field are effectively cancelled and the resulting 810 nm state has a high fidelity to the initial vacuum state (Fig. 5(d)). The residual phase quadrature noise in Fig. 5(d) is less than 0.07 QNL and we attribute this noise mainly to the nonideal cavity locking of the two DFGs. The different cavity length fluctuations will modulate the pump phases in different ways and result in slightly different phase fluctuations for the two pump fields which cannot be cancelled completely.

Above results verify that if one transforms only the signal field (in this case the self-homodyne measurements by a frequency-dependent reflection of the optical field [27–29] can be used to measure the field quadratures), the phase fluctuations of the pump field can lead to increase of noise in the phase quadrature of the down-converted field. However, the influence of the pump phase noise can be eliminated effectively by transforming both the signal field and the corresponding LO where the same noisy pump field is adopted (in this case BHD can be used to measure the field quadratures).

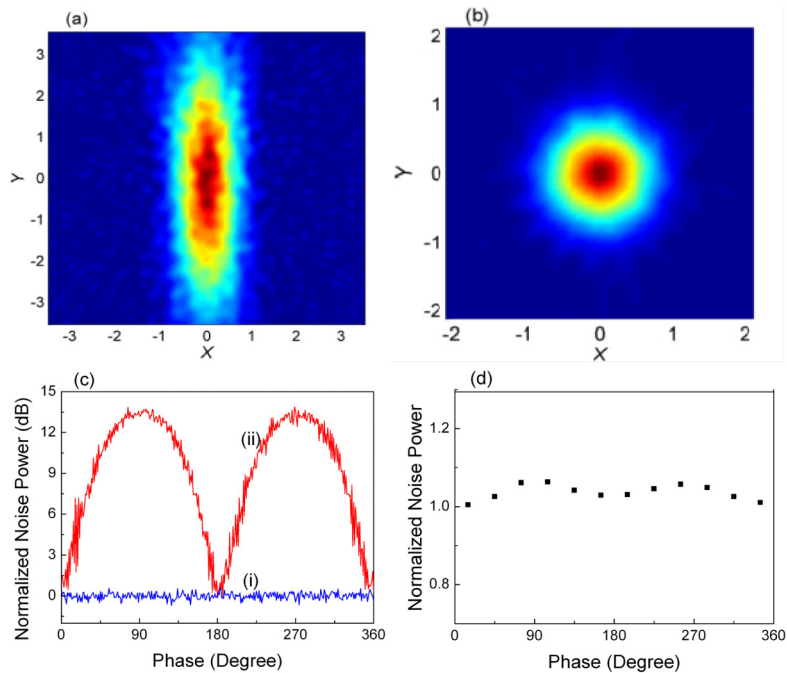


Fig. 5. Wigner functions of the frequency down-converted 810 nm quantum state when only the pump field of the DFG1 is phase modulated (a), and the pump fields of the two DFGs are phase modulated simultaneously (b). The corresponding quadrature noise power is displayed in (c) and (d), (i) Quantum noise limit; (ii) Quadrature noise power.

5. Conclusion

In conclusion, high efficiency and low noise quantum frequency down-conversion of a bright amplitude-squeezed state was achieved via a cavity-enhanced DFG process. The influence of amplitude and phase fluctuations of the pump field on the frequency conversion of bright CV quantum states is analyzed in depth, both theoretically and experimentally. It is shown that by operating the DFG at exactly the optimal conversion point and employing a dual DFG in

which common pump field is adopted the QFC is insensitive to the small amplitude and phase noises of the pump field. The demonstrated scheme provides an effective way for faithful frequency conversion of bright CV quantum state with noisy pump field, and can be applied to the frequency conversion of Einstein-Podolsky-Rosen entangled states and other complex quantum states which are useful in quantum communication and quantum metrology.

Acknowledgments

This research is supported by the National Science Foundation of China (NSFC) (11074156, 61378010), the National Key Basic Research Program of China (2010CB923101), the NSFC Project for Excellent Research Team (61121064), the Natural Science Foundation of Shanxi Province (2014011007-1).